Bioorganic Chemistry 112 (2021) 104904

Contents lists available at ScienceDirect

Bioorganic Chemistry

journal homepage: www.elsevier.com/locate/bioorg

Design, synthesis and biological evaluation of novel imidazole-chalcone derivatives as potential anticancer agents and tubulin polymerization inhibitors

Sara Rahimzadeh Oskuei [a,b,1], Salimeh Mirzaei [c,1], Mohammad Reza Jafari-Nik [b], Farzin Hadizadeh [a,b], Farhad Eisvand [d], Fatemeh Mosaffa [a], Razieh Ghodsi [a,b,*]

[a] Biotechnology Research Center, Mashhad University of Medical Sciences, Mashhad, Iran
[b] Department of Medicinal Chemistry, School of Pharmacy, Mashhad University of Medical Sciences, Mashhad, Iran
[c] Department of Medicinal Chemistry, Faculty of Pharmacy, Hormozgan University of Medical Sciences, Bandar Abbas, Iran
[d] Department of Toxicology, School of Pharmacy, Mashhad University of Medical Sciences, Mashhad, Iran

ARTICLE INFO

Keywords:
Chalcone
Imidazole
Tubulin inhibitors
Anticancer activity
Molecular docking
Apoptosis

ABSTRACT

Novel imidazole-chalcone derivatives were designed and synthesized as tubulin polymerization inhibitors and anticancer agents. The antiproliferative activity of the imidazole-chalcone was assessed on some human cancer cell lines including A549 (adenocarcinoma human alveolar basal epithelial cells), MCF-7 (human breast cancer cells), MCF-7/MX (mitoxantrone resistant human breast cancer cells), and HEPG2 (human hepatocellular carcinoma cells). Generally, the imidazole-chalcone derivatives exhibited more cytotoxicity on A549 cancer cells in comparison to the other three cell lines, among them compounds 9j' and 9g showed significant cytotoxicity with IC_{50} values ranging from 7.05 to 63.43 μM against all the four human cancer cells. The flow cytometry analysis of A549 cancer cells treated with 9g and 9j' displayed that these compounds induced cell cycle arrest at the G2/M phase at low concentrations and increased the number of apoptotic cells (cells in subG1 phase) at higher concentrations. They have also inhibited tubulin polymerization similar to combretastatin A-4 (CA-4). Annexin V binding staining assay in A549 cancer cells revealed that compound 9j' induced apoptosis (early and late). Finally, molecular docking studies of 9j' into the colchicine-binding site of tubulin presented the probable interactions of these compounds with tubulin.

1. Introduction

Cancer is a multifactorial disease and considered one of the most serious illnesses worldwide. Although the biological pathways involved in cancer became more clear over time, potent and effective anticancer drugs are needed for the treatment of cancer. The existing anticancer agents formulated from natural and synthetic products exert toxicity due to the low site-specificity, which leads to healthy cell damage and drug resistance [1–3].

Microtubules, comprising α-β tubulin heterodimer, are important components of the eukaryotic cytoskeleton. They control several cellular functions including motility regulation, cell signaling, secretion, cell architecture in interphase [4–6]. Since microtubules have an important role in the life cycle of the cell, they have been recognized as major targets for the development of novel anticancer compounds recently [7–17] There are three well known binding sites in tubulin including the vinca domain, colchicine, and paclitaxel sites [18,19]. Numerous antimitotic agents are derived from both natural and synthetic sources. Anti-mitotic agents such as taxanes and vinca alkaloids have been utilized for the clinical treatment of different cancerous patients in the last decades [4,19]. However, high toxicity, poor solubility, low oral bioavailability render these agents less optimum for clinical treatment of cancer [20] Therefore, scientists are encouraged to develop novel antimitotic agents in order to overcome the mentioned drawbacks.

Chalcones are essential pharmacophores of many natural products such as curcumin, flavokawain, millepachine, and xanthohumol [21]. Chalcone-based derivatives have received notable attention because of their wide ranges of biological activities, such as anti-oxidant, antibacterial, anti-fungal, anti-proliferative [22–25], and antidiabetic activities [26]. Over the last few years, many attempts have been done for

* Corresponding author.
[1] These authors contributed equally in this study.

https://doi.org/10.1016/j.bioorg.2021.104904
Received 5 January 2021; Received in revised form 3 April 2021; Accepted 7 April 2021
Available online 20 April 2021

the development of chalcone derivatives as tubulin polymerization inhibitors such as chalcone 1 and compounds **A-D** (Fig. 1) [15,23,27–36]. It is reported that chalcones may act as Michael acceptors and alkylate numerous critical proteins of the tubulin-microtubule system [37], thereby chalcone has been considered as an advantaged scaffold for the design and development of new anti-cancer agents [31]. Some imidazole derivatives also are reported as tubulin inhibitors such as compounds **E-G** (Fig. 1) [22,38–41]. On the other hand, many studies demonstrated that natural products possessing imidazole ring which are derived from marine including eleutherobin, sarcodictyin A, sarcodictyin B (Fig. 1), exhibit tubulin inhibition activity [42]. The biological importance and relative shortage of these natural products have prompted several groups to undertake the total chemical synthesis of these products and their derivatives. They reported the structure-activity relationships derived from these studies. The most noticeable result was the significant role of the α, β–unsaturated hetero-aromatic side chain for both antiproliferative activities and tubulin binding. Moreover, the natural imidazole ring displayed the optimal activity, whereas replacing the imidazole ring with other aromatic rings such as pyridine, thiazole, or oxazole led to a decrease in activity [43]. Therefore, according to these findings, in this study new imidazole-chalcone derivatives are designed and synthesized as tubulin inhibitors. The rationale for the design of the imidazole-chalcone hybrids is represented in Fig. 1. The antiproliferative activity of synthesized compounds was evaluated against four different cancer cell lines including A549 (adenocarcinoma human alveolar basal epithelial cells), MCF-7 (human breast cancer cells), MCF-7/MX (mitoxantrone resistant human breast cancer cells), and HEPG2 (human hepatocellular carcinoma cells). Compounds that displayed the most antiproliferative activity were examined for their effects on induction of apoptosis and cell cycle arrest using flow cytometry, these compounds were also evaluated to inhibit microtubule polymerization. Besides, to describe the obtained results of biological assessments, docking studies were performed.

2. Results and discussion:

2.1. Synthesis

Compounds **7a** and **7b** were synthesized using the procedures reported before [44] As illustrated in Scheme 1, benzyl amine (1), dihydroxyacetone (2) and potassium thiocyanate (3) in a solution of acetic acid and 1-butanol were stirred for 72 h to afford (1-benzyl-2-mercapto-1H-imidazol-5-yl) methanol (4). Then methyl iodide or ethyl iodide was added to a solution of compound **4** in methanol in the presence of an aqueous solution of sodium hydroxide to produce compounds **5** and **6**. These compounds (5 and 6) were oxidized by magnesium dioxide (MnO_2) under reflux conditions with chloroform to afford compound **7**. Finally, Compounds **9a-9j'** were synthesized by applying Claisen-Schmidt condensation between compound **7a** or **7b** and different acetophenones (**8a-8j)** in the presence of the methanolic sodium hydroxide. Oxidation of **9j** with oxone in THF-water gave the oxidized methylsulfonyl compound **9k**. The structures of compounds were confirmed by nuclear magnetic resonance (^{1}HNMR, ^{13}C NMR) and mass spectrometry.

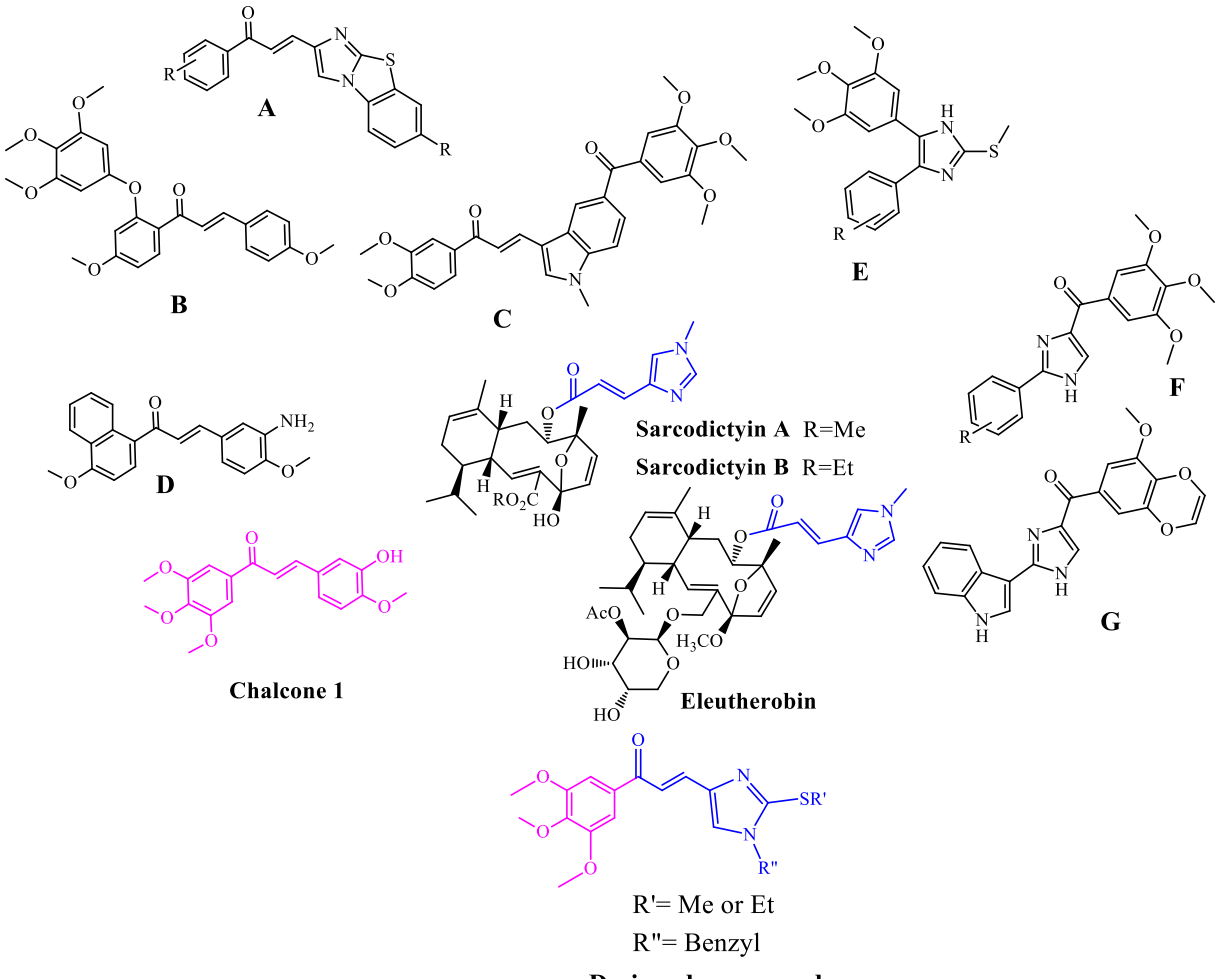

Fig. 1. Chemical structures of known tubulin inhibitors and our designed compounds.

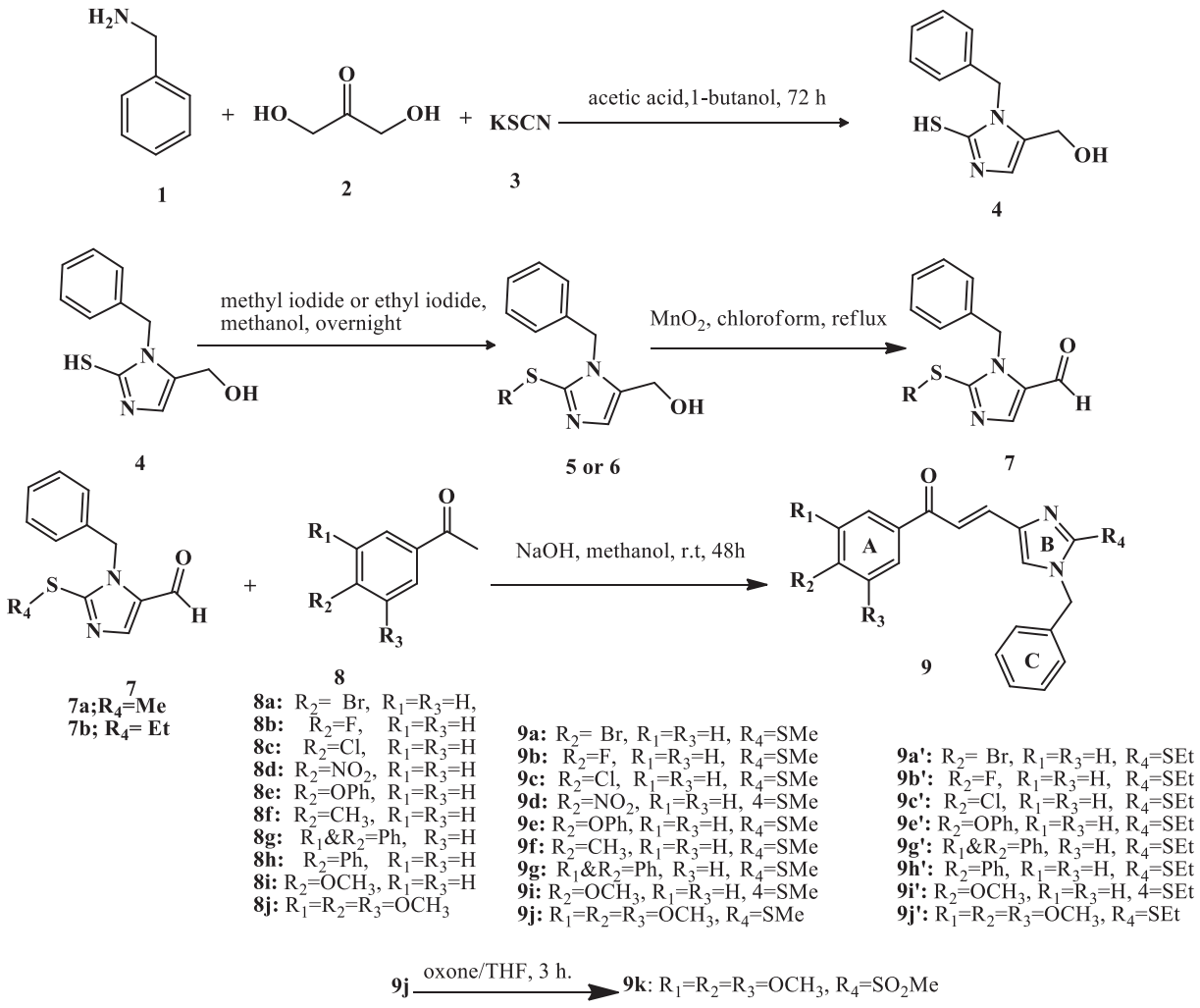

Scheme 1. Reagents and conditions.

2.2. Biological evaluation

2.2.1. In vitro anticancer activity

To evaluate the cytotoxic effects of these newly imidazole-chalcone derivatives, MTT assay was performed against four cancer cell lines including A549 (adenocarcinoma human alveolar basal epithelial cells), MCF-7 (human breast cancer cells), MCF-7/MX (mitoxantrone resistant human breast cancer cells), and HEPG2 (human hepatocellular carcinoma cells) using combretastatin A-4 (CA-4) as the positive control. As shown in Table 1, most of our compounds exhibited moderate to high antiproliferative activity, with IC_{50} values in the micromolar range. Generally, the imidazole-chalcone derivatives showed more cytotoxicity on A549 cancer cells in comparison to the other three cell lines. HEPG2 cancer cells were not so sensitive to our compounds except **9j'**. Among the synthesized compounds, **9j'** and **9g** displayed significant cytotoxicity with IC_{50} values ranging from 7.05 to 63.43 μM against all four human cancer cells. Compound **9j'** possessing three methoxy groups on A-ring (Scheme 1**)** demonstrated stronger activity than the other compounds, since trimethoxyphenyl moiety is an important pharmacophore in some strong tubulin inhibitors such as CA-4, the increased activity of 9j' is likely due to the extensive interactions of the trimethoxyphenyl group with tubulin. Based on the IC_{50} values of the synthesized compounds, compounds **9g** and **9g'** possessing naphthalene group, showed an acceptable potency with IC_{50} values of 11.7 μM and 13.96 μM on A-549 cell line, and 14.4 μM and 24.07 μM on MCF7/MX cell line, respectively. This may be due to their ability to penetrate the cell membrane because of their increased lipophilicity or enhanced interactions with residues in the active site of tubulin [45–50]. It is also concluded that the higher cytotoxic activity of non-polar compounds could be attributed to their higher lipophilicity leading to better permeability to lipophilic cell membranes. Compounds **9h** and **9h'** have less cytotoxicity than compounds **9g** and **9g'**, despite having a phenyl group at position 4 (C-4) of A-ring. This may be because of the steric hindrance of the phenyl ring in the active site of tubulin.

Compound **9a** possessing bromine atom (Br) at position 4 (C-4) of A-ring displayed strong cytotoxic activity against A549 cancer cells, comparable to the most potent compound **9j'**, which may be due to the proper size and lipophilicity of the bromine (Br). Replacing Br with chlorine and fluoride reduced the potency of the compound. Oxidizing compound **9j** increased the cytotoxicity of this compound on MCF-7 (compare the cytotoxicity of **9k** with its parent **9j**). Clog P (Calculated logP) is an important factor in membrane permeability and hence antiproliferative activity. Clog values of the compounds also were determined [51]. These compounds had ClogP values in range of 2.48–4.01 (Table 1). As shown in Table 1, in general, there is not a significant correlation between ClogP values and MTT data in our compounds.

2.2.2. Tubulin polymerization assay

Based on the acquired antiproliferative activities of imidazole-chalcone hybrids on human cancer cells, **9j'** and **9g** (the most potent antiproliferative compounds) and **9j (**which did not show significant

Table 1

The in vitro antiproliferative activities (IC_{50} (μM)[a]) of compounds 9a-9j' against human cancer cell lines.

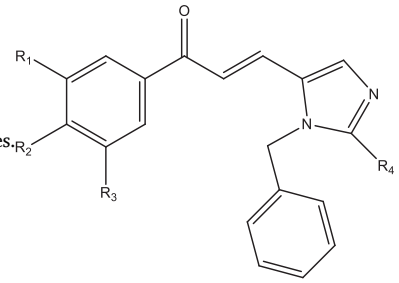

Compound	R_1	R_2	R_3	R_4	A-549	MCF-7	HEPG 2	MCF-7 MX	Clog P
9a	H	Br	H	SCH_3	8.84 ± 2.31	27.94 ± 3.41	66.35 ± 3.76	85.63 ± 4.89	3.44
9b	H	F	H	SCH_3	13.31 ± 2.12	17.53 ± 3.11	>100	22.14 ± 2.74	3.19
9c	H	Cl	H	SCH_3	>100	29.08 ± 3.17	51.71 ± 4.15	>100	3.31
9d	H	N_2O	H	SCH_3	87.02 ± 5.34	>100	>100	>100	2.77
9e	H	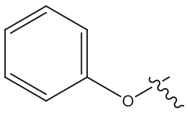	H	SCH_3	14.87 ± 3.66	28.3 ± 3.55	>100	29.75 ± 2.44	3.55
9f	H	CH_3	H	SCH_3	26.01 ± 3.44	21.24 ± 2.53	>100	32.89 ± 3.15	3.04
9g			H	SCH_3	11.7 ± 1.62	14.85 ± 2.73	63.43 ± 5.33	14.94 ± 1.91	3.41
9i	H	OCH_3	H	SCH_3	>100	28.3 ± 2.78	ND	ND	3.42
9j	OCH_3	OCH_3	OCH_3	SCH_3	66.47 ± 4.85	>100	>100	54.86 ± 2.94	3.76
9k	OCH_3	OCH_3	OCH_3	SO_2CH_3	ND	18.33 ± 3.15	>100	>100	2.48
9a'	H	Br	H	S-Ethyl	78.9 ± 4.87	14.6 ± 2.14	>100	>100	3.35
9b'	H	F	H	S-Ethyl	85.42 ± 5.76	>100	>100	17.4 ± 2.66	3.44
9c'	H	Cl	H	S-Ethyl	>100	76.13 ± 3.77	>100	>100	3.39
9e'	H	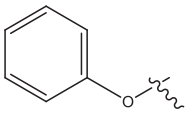	H	S-Ethyl	17.89 ± 2.44	33.42 ± 2.94	>100	>100	4.01
9g'			H	S-Ethyl	13.96 ± 2.48	>100	>100	24.07 ± 3.56	3.59
9h'	H	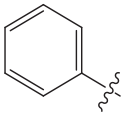	H	S-Ethyl	>100	>100	>100	>100	3.88
9i'	H	OCH_3	H	S-Ethyl	>100	33.42 ± 3.46	ND	ND	3.71
9j'	OCH_3	OCH_3	OCH_3	S-Ethyl	7.05 ± 1.12	9.88 ± 1.56	21.97 ± 2.23	20.2 ± 2.76	3.86
CA4					0.86 ± 0.23	0.43 ± 0.14	0.63 ± 0.17	1.49 ± 0.47	3.61

[a] Compound concentration required to inhibit the cells growth by 50%. ND; not determined.

antiproliferative activity) were assessed for in vitro inhibitory effects on tubulin polymerization at 50 and 100 μM concentrations. In this evaluation, compounds paclitaxel, (a polymerization promoter), and CA-4, (a polymerization suppressor), were used as the references. As shown in Fig. 2, 9j' at the concentrations of 50 and 100 μM inhibited tubulin polymerization by 42.85% and 60.71% respectively, and **9g** inhibited tubulin polymerization by 25% and 55.71% at the concentrations of 50 and 100 μM, respectively. The tubulin inhibitory activity of Compound **9j** was less than those of **9j**' and **9g** which is consistent with their antiproliferative activities as well. inhibited The results confirmed that these compounds are able to inhibit tubulin polymerization in a dose-dependent manner and in a mode similar to that of CA-4 (5 μM). These data revealed that one of the mechanisms of antiproliferative activity of these compounds may be due to inhibition of tubulin polymerization.

2.2.3. Cell cycle analysis using flow cytometry

Antimitotic drugs, by the destruction of the microtubular network, induce cell cycle arrest at the G2/M phase. To investigate the mechanism of cytotoxicity of compounds **9j'** and **9g**, the effects of these compounds at different concentrations on the cell cycle progression of A549 cells were evaluated by flow cytometry. Since cell cycle arrest causes DNA fragmentation, the percentage of sub-G1 apoptotic cells in cancer cells treated with compounds **9j'** and **9g**, was measured. As displayed in Figs. 3 and 4, treatment of A549 cells with **9j'** (10, 20, and 40 μM) for 48 h, induced cell cycle arrest at G2/M phase and increased the percentage of cells from 14.11% in the control group to 34.9% at the concentration of 10 μM, but at higher concentrations, the cells number at sub-G1 phase increased, which indicating the cells were subjected to apoptosis when treated by higher concentrations. when A549 cell line was treated with **9g** at various concentrations for 48 h, the percentages of cells in the G2/M phase were 29.78% and 32.92% at concentrations of 10 μM and 20 μM (in comparison to 14.11% arrested cells in the control group), at 40 μM concentration the percentage of cells in the subG1 phase was increased. These results further confirmed that **9j'** and **9g** possibly exerted their antiproliferative activity through cell cycle arrest at the G2/M phase and finally induction of cellular apoptosis.

2.2.4. Apoptosis assay

Compound **9j**' was evaluated by Annexin V FITC/PI (AV/PI) dual staining assay to characterize the mode of cell death induced by these compounds. This assay can detect between live cells (Q4), early

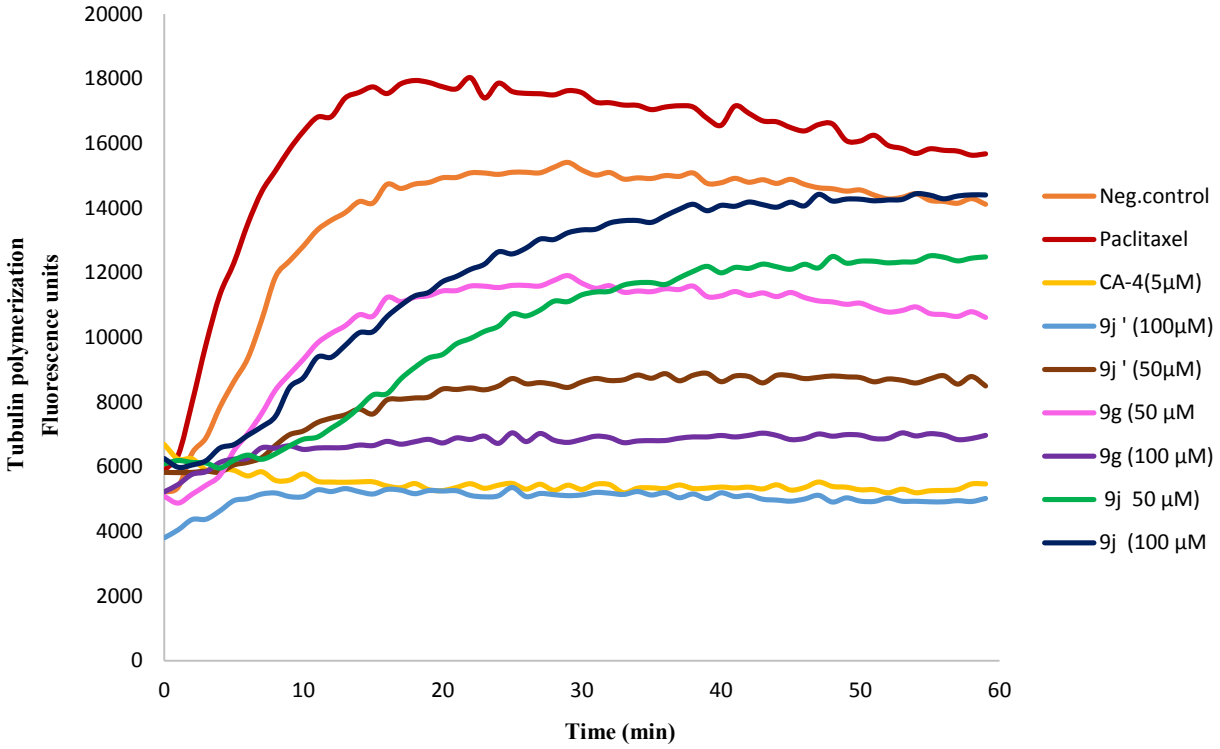

Fig. 2. Effects of compounds **9g, 9j'** and **9j** on in vitro tubulin polymerization.

apoptotic cells (Q3), late apoptotic cells (Q2), and necrotic cells (Q1). In this study A549 cells were treated with **9j'** for 24 h at 10, 20, and 40 μM concentrations (Fig. 5). The results showed an accumulation of total apoptotic cells (early and late apoptotic cells) from 3.1% (in untreated control) to 11.54% (10 μM), 50.7% (20 μM), and 54.2% (40 μM), respectively (Fig. 5). The findings indicated that **9j'** can induce cellular apoptosis (in a dose-dependent manner) and these results are consistent with its antiproliferative effect in the tested cell lines.

2.3. Molecular modeling studies

To investigate the possible binding mode of the synthesized imidazole-chalcone hybrids with tubulin, docking studies of these compounds were performed at the colchicine binding site of the tubulin crystal structure (PDB ID: 4O2B) using MOE 2015.10.

All the synthetic compounds were well accommodated inside the colchicine binding site of tubulin. The docking pose of **9j'**, the most potent compound in the series, in complex with tubulin was shown in Figs. 6 and 7. Compound **9j'**, has shown two hydrogen bond interactions with the catalytically active residues Ser 178α and Ala 316β and (red dashed line in Fig. 6A) a cation-π interaction with Asn 258β (Fig. 6A). Further, several hydrophobic interactions between the compound **9j'** and other residues, such as Glu183α, Thr 224α, Lys 254β, Asn 101α, Val 351β, Lys 352β, and Leu 248β were observed (Fig. 6B). These various hydrophobic interactions and hydrogen bonds formation of 9j' with tubulin can describe the inhibitory effect of this compound.

3. Conclusion

In the current study, a new series of imidazole-chalcone hybrids were synthesized as tubulin inhibitors. The cytotoxic activity of the synthesized compounds was evaluated against four cancer cell lines including MCF7, A549, HepG2, and MCF7/MX by MTT assay. Generally, the imidazole-chalcone derivatives displayed more cytotoxicity on A549 cancer cells in comparison to the other three cell lines, among them, **9j'** and **9g** exhibited strong cytotoxic activity with IC_{50} values ranging from 7.05 to 63.43 μM against all four human cancer cells. Compound **9j'** possessing three methoxy groups on A-ring exhibited potent antiproliferative activity against all cancer cells, which's in agreement with the potent tubulin inhibitors with trimethoxyphenyl pharmacophore such as CA-4. The flow cytometry analysis of A549 cancer cells treated with **9g** and **9j'** showed that low concentrations of these compounds induced cell cycle arrest at the G2/M phase, while at higher concentrations they increased the number of apoptotic cells (cells in subG1 phase). Annexin V-FITC/PI staining assay in A549 cancer cells treated with **9j'** displayed that **9j'** induced cell apoptosis in a dose-dependent manner. Besides, compounds **9j'** and **9g**, inhibited tubulin polymerization similar to CA-4. Finally, molecular docking studies of **9j'** into the colchicine binding site of tubulin demonstrated the probable interactions of this compound with tubulin.

4. Experimental

4.1. Chemistry

All needed reagents were bought from Merck and Acros. The progress of all reactions was monitored using thin-layer chromatography (TLC) with 0.25 mm silica gel plates (60 GF-254- Merck & Co (Darmstadt, Germany)). Melting points were measured by a Thomas Hoover capillary instrument. NMR spectra were acquired using a Bruker FT-300 MHz instrument. Compounds were solved in Chloroform-D or DMSO-D6 before acquiring NMR spectra. Coupling constant (J) values were measured in hertz (Hz) and spin multiples are given as s (singlet), d (doublet), t (triplet), q (quartet), m (multiplet). The mass spectra were acquired using a 3200 QTRAP LC/MS triple quadrupole mass spectrometer possessing an electrospray ionization (ESI) interface.

4.2. General procedure for the synthesis of 3-(1-benzyl-2-(methylthio or ethylthio)-1H-imidazol-4-yl)-1-phenylpropan-1-one (9a-9j')

An aqueous solution of sodium hydroxide 2 N (2 ml) was added to 1-benzyl-2-mercapto-1H-imidazole-5-carbaldehyde derivatives (**7a** or **7b**,

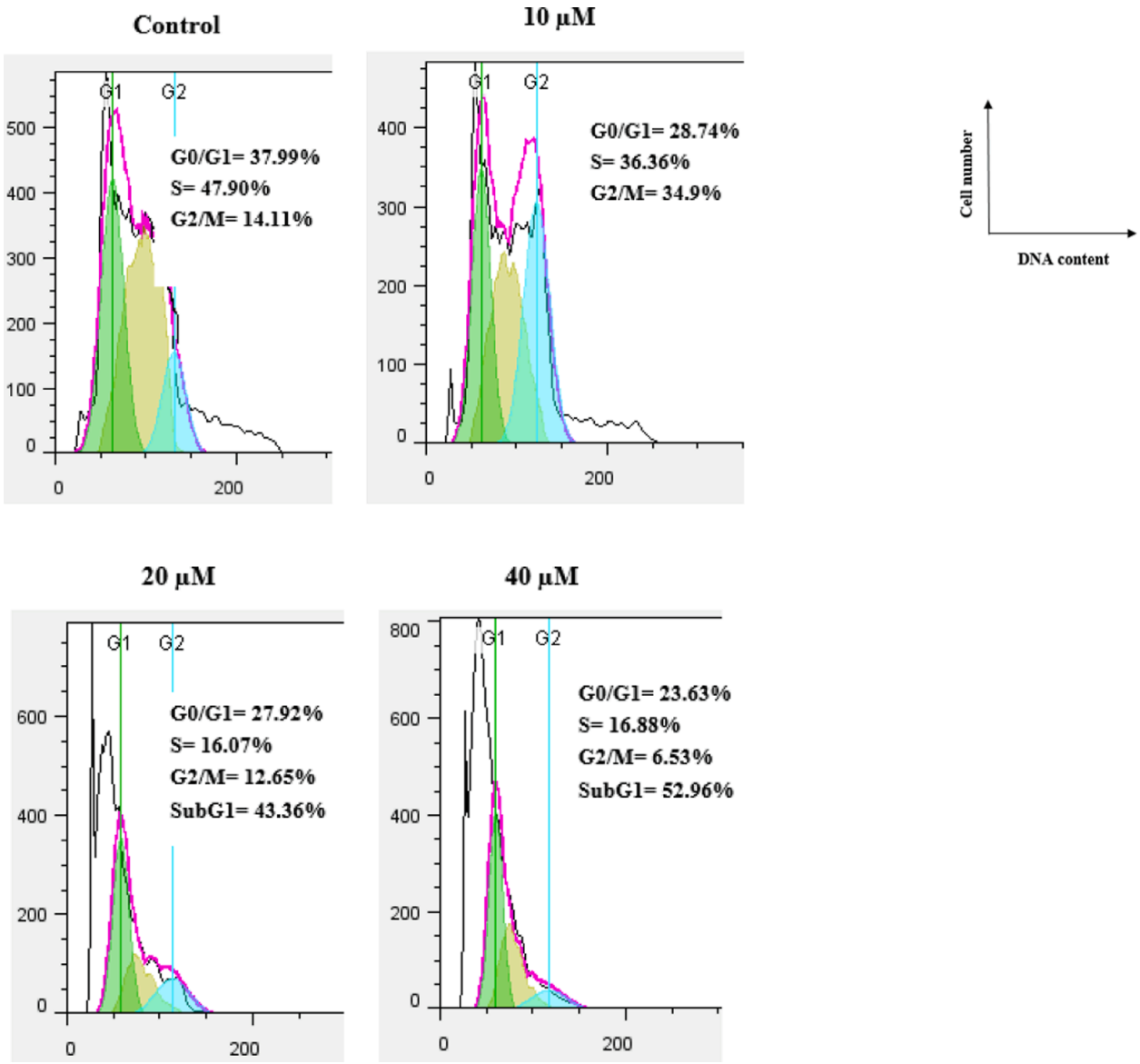

Fig. 3. Flow cytometry analysis of compound **9j'** in A549 cancer cells.

1 mmol) in methanol (5 ml), then the appropriate acetophenone (**8a-8j**, 1 mmol) was added to the mixture and was stirred at room temperature for 24–48 h (monitored by TLC). Upon completion, HCl (2 N) was added until a precipitate formed. The crude product was filtrated, washed with cold ethanol and recrystallized in methanol.

4.2.1. (E)-3-(1-benzyl-2-(methylthio)-1H-imidazol-4-yl)-1-(4-bromophenyl) prop-2-en-1-one (9a)

Yield: 62%; mp = 203–205 °C; ^{1}HNMR (300 MHz-DMSO-d_6): δ (ppm) 2.80 (s, 3H, SCH_3), 5.55 (s, 2H, CH_2), 7.15–7.18 (m, 2H, ArH), 7.31–7.44 (m, 3H, ArH), 7.53–7.58 (d, 1H, CH = CH, J = 15.3 Hz), 7.77–7.79 (d, 2H, 4-bromophenyl, H_2 &H_6, J = 8.7 Hz), 7.87–7.92 (d, 1H, CH = CH, J = 15.3 Hz), 7.97–8.00 (d, 2H, 4-bromophenyl, H_3 &H_5, J = 8.7 Hz), 8.50 (s, 1H, imidazole); ^{13}CNMR (75 MHz-DMSO-d_6): δ (ppm) 16.34, 48.23, 122.381, 126.87, 128.06, 128.55, 128.60, 129.52, 130.88, 131.88, 132.38, 135.63, 136.58, 147.42; LC-MS [52]: 414.3 $(M + H)^+$.

4.2.2. (E)-3-(1-benzyl-2-(ethylthio)-1H-imidazol-4-yl)-1-(4-bromophenyl) prop-2-en-1-one (9a')

Yield: 75%; mp = 153–155 °C; ^{1}HNMR (300 MHz-DMSO-d_6): δ (ppm)1.25–1.30 (t, 3H, CH_3, J = 7.2 Hz), 3.29–3.36 (SCH_2, J = 7.2 Hz), 5.57 (s, 2H, CH_2), 7.13–7.16 (m, 2H, ArH), 7.31–7.42 (m, 3H, ArH), 7.53–7.58 (d, 1H, CH = CH, J = 15.3 Hz), 7.74–7.78 (d, 2H, 4-bromophenyl, H_2 &H_6, J = 8.7 Hz), 7.89–7.94 (d, 1H, CH = CH, J = 15.3 Hz), 7.98–8.01 (d, 2H, 4-bromophenyl, H_3 &H_5, J = 8.7 Hz), 9.62 (s, 1H, imidazole); ^{13}CNMR (75 MHz-DMSO-d_6): δ (ppm), 15.04, 28.77, 48.31, 126.77, 127.19, 128.06, 128.51, 128.64, 129.49, 130.89, 132.00, 132.36, 135.76, 136.55, 145.59, 187.75; LC-MS [52]: 427.3 $(M + H)^+$.

4.2.3. (E)-3-(1-benzyl-2-(methylthio)-1H-imidazol-4-yl)-1-(4-fluorophenyl) prop-2-en-1-one (9b)

Yield: 42%; mp = 183–185 °C; ^{1}H NMR (300 MHz-DMSO-d_6): δ (ppm) 2.64–2.65 (s, 3H, CH_3, J = 4.5 Hz), 5.40 (s, 2H, CH_2), 7.08–7.11 (d, 2H, ArH, J = 8.4 Hz), 7.28–7.37 (m, 3H, ArH), 7.39–7.42 (m, 2H, ArH), 7.52–7.57 (d, 1H, HC = CH, J = 15.6 Hz), 7.64–7.70 (d, 1H, HC = CH, J = 15.6 Hz), 8.05 (s, 1H, imidazole), 8.07–8.09 (d, 1H, ArH, J = 5.4 Hz), 8.10–8.12 (d, 1H, ArH, J = 5.7 Hz); ^{13}CNMR (75 MHz-DMSO-d_6): δ (ppm) 15.47, 47.36, 116.06 (CF), 116.34 (CF), 118.85, 126.44, 128.18, 129.40, 129.87, 131.54, 131.64, 134.26, 134.78, 136.81, 148.55; LC-MS (ESI): 353.4 $(M + H)^+$, 375.5 $(M + Na)^+$.

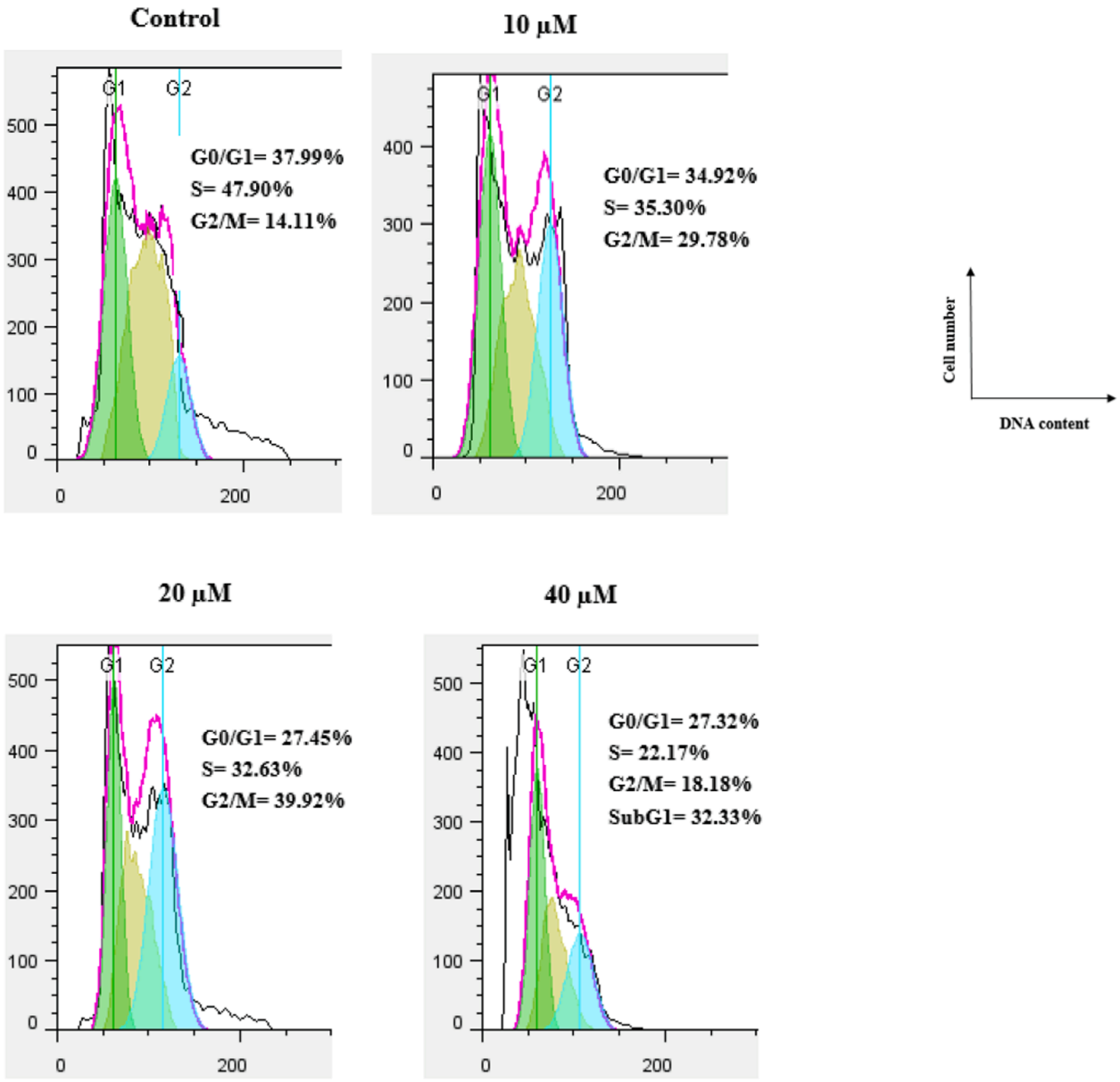

Fig. 4. Flow cytometry analysis of compound **9g** in A549 cancer cells.

4.2.4. (E)-3-(1-benzyl-2-(ethylthio)-1H-imidazol-4-yl)-1-(4-fluorophenyl) prop-2-en-1-one (9b')

Yield: 41%; mp = 134–136 °C; ^{1}H NMR(300 MHz-DMSO-d_6): δ (ppm) 1.28–1.32 (t, 3H, CH_3, J = 14.4 Hz), 3.14–3.21 (q, 2H, CH_2, J = 7.2), 5.42 (s, 2H, CH_2), 7.07–7.09 (d, 2H, ArH, J = 6.9 Hz), 7.28–7.41 (m, 5H, ArH), 7.51–7.56 (d, 1H, HC = CH, J = 15.6 Hz), 7.65–7.70 (d, 1H, HC = CH, J = 15.3 Hz), 8.06 (s, 1H, imidazole), 8.07–8.09 (d, 1H, ArH, J = 5.4 Hz), 8.10–8.12 (d, 1H, ArH, J = 5.7 Hz); 15.53, 27.85, 47.38, 118.56, 126.56, 128.16, 129.39, 130.17, 130.58, 131.39, 134.55, 136.73, 136.90, 138.37, 147.53, 187.63; LC-MS(ESI): 367.4 $(M + H)^+$.

4.2.5. (E)-3-(1-benzyl-2-(methylthio)-1H-imidazol-4-yl)-1-(4-chlorophenyl) prop-2-en-1-one (9c)

Yield: 59%; mp = 183–1855 °C; ^{1}H NMR(300 MHz-DMSO-d_6): δ (ppm) 2.69 (s, 3H, CH3), 5.46–5.50 (s, 2H, CH_2), 7.12–7.17 (t, 2H, ArH), 7.29–7.46 (m, 3H, ArH), 7.56–7.66 (t, 3H, ArH), 7.71–7.77 (d, 1H, HC = CH, J = 15.6 Hz), 8.03–8.08 (m, 2H, ArH), 8.20 (s, 1H, imidazole); LC-MS(ESI): 369.4 $(M + H)^+$.

4.2.6. (E)-3-(1-benzyl-2-(ethylthio)-1H-imidazol-4-yl)-1-(4-chlorophenyl) prop-2-en-1-one (9c')

Yield: 63%; mp = 148–150 °C; ^{1}H NMR(300 MHz-DMSO-d_6): δ (ppm) 1.27–1.32 (t, 3H, CH_3, J = 7.2 Hz), 3.14–3.21 (q, 2H, CH_2, J = 7.3 Hz), 5.42 (s, 2H, CH_2), 7.06–7.09 (d, 2H, ArH, J = 7.2 Hz), 7.27–7.32 (t, 1H, ArH, J = 7.2 Hz), 7.36–7.41 (t, 2H, ArH, J = 7.2 Hz), 7.52–7.57 (d, 1H, HC = CH, J = 15.6 Hz), 7.59–7.62 (d, 2H, ArH, J = 8.7 Hz), 7.63–7.68 (d, 1H, HC = CH, J = 15.6 Hz), 8.00–8.03 (d, 2H, ArH, J = 8.7 Hz), 8.07 (s, 1H, imidazole); ^{13}CNMR(75 MHz-DMSO-d_6): δ (ppm) 15.63, 27.58, 47.38, 118.56, 126.56, 128.16, 129.30, 130.17, 130.58, 131.39, 134.55, 136.73, 136.90, 138.37, 147.53, 187.63; LC-MS (ESI): 383.4 $(M + H)^+$.

4.2.7. (E)-3-(1-benzyl-2-(methylthio)-1H-imidazol-4-yl)-1-(4-nitrophenyl)prop-2-en-1-one (9d)

Yield: 12%; mp = 165–167 °C; ^{1}HNMR(300 MHz-DMSO-d_6): δ (ppm) 2.72 (s, 3H, SCH_3), 5.48 (s, 2H, CH_2), 7.12–7.14 (m, 2H, ArH), 7.30–7.43 (m, 3H, ArH), 7.57–7.62 (d, 1H, CH = CH, J = 15.3 Hz), 7.77–7.78 (d, 1H, CH = CH, J = 15.3 Hz), 8.21–8.34 (m, 5H, ArH); ^{13}CNMR(75 MHz-

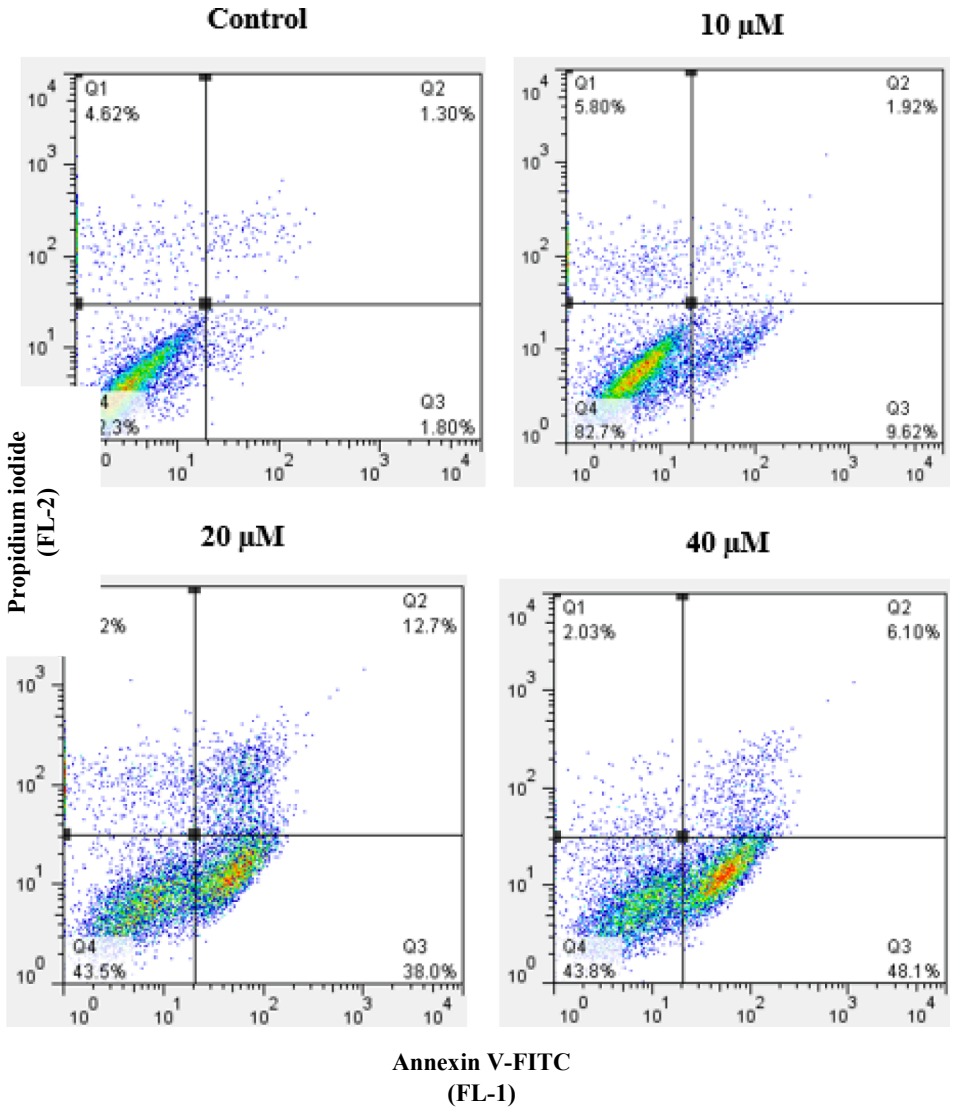

Fig. 5. Effects of **9j'** on the apoptosis of A549 cancer cells after 24 h using annexin V/PI double staining test by flow cytometry.

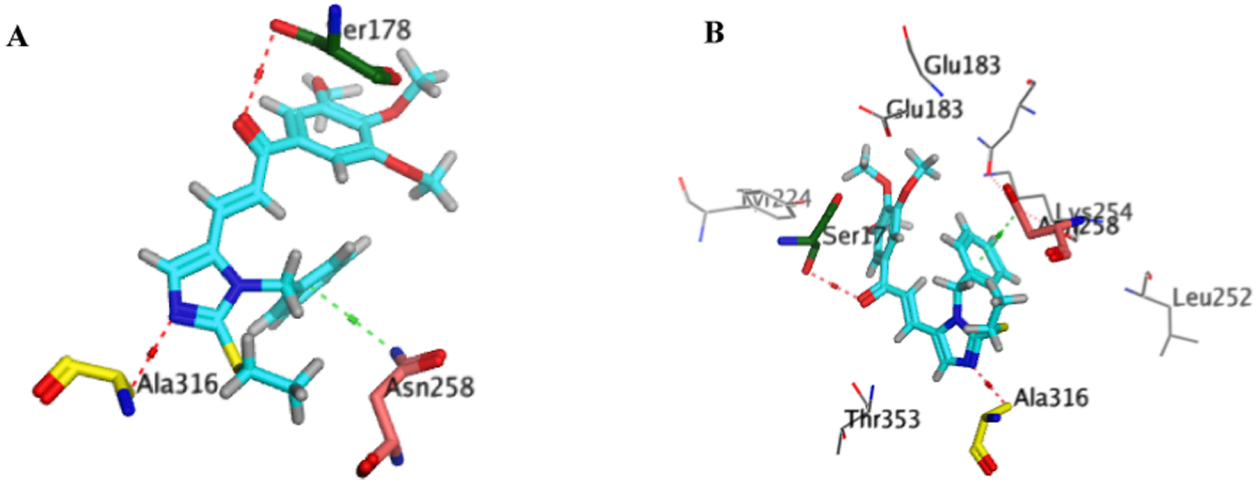

Fig. 6. Binding mode of **9j'** in colchicine binding site. A) Hydrogen bonding of **9j'** with colchicine binding site of tubulin (red dashed line). B) Hydrophobic interactions of **9j'** with tubulin. (For interpretation of the references to colour in this figure legend, the reader is referred to the web version of this article.)

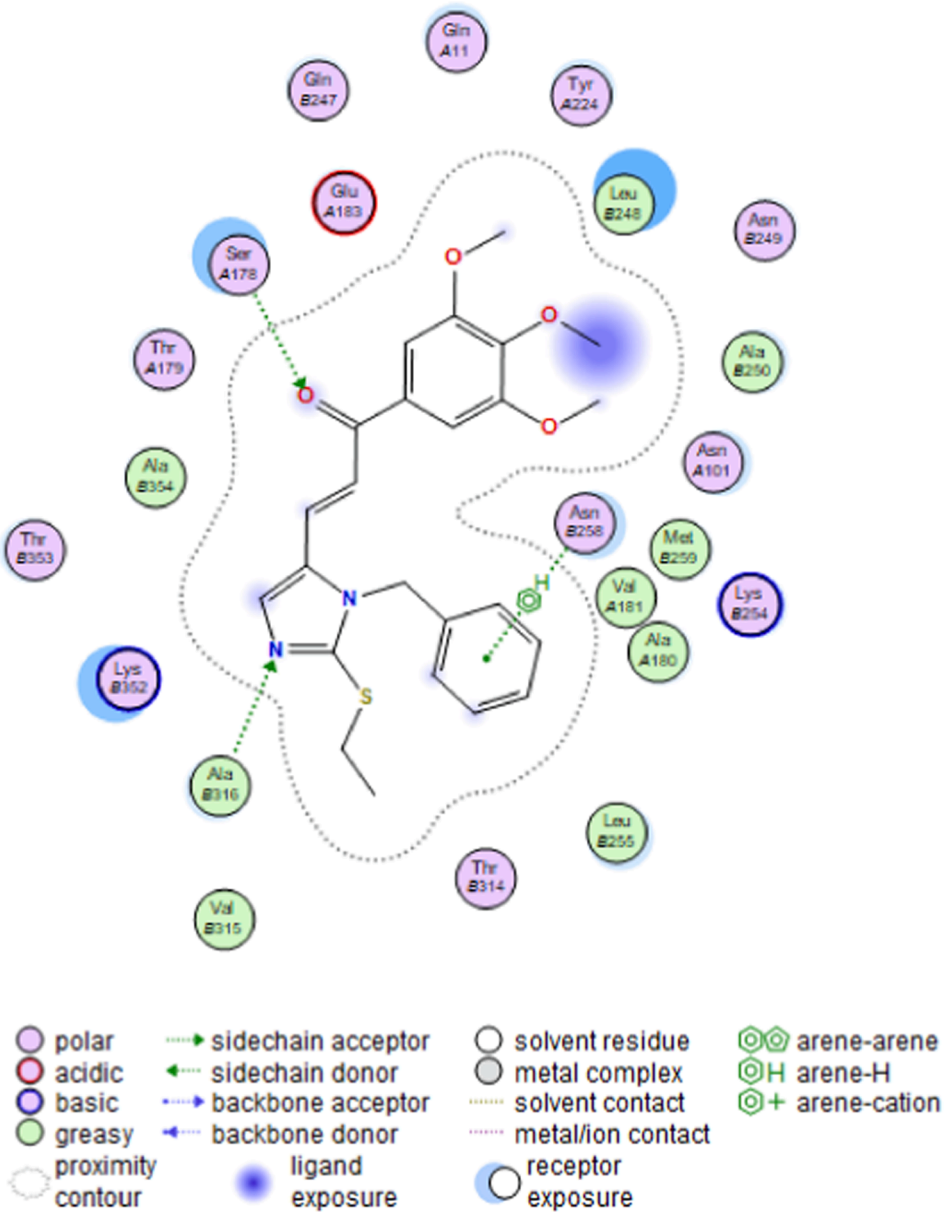

Fig. 7. The 2D representation of the interaction between compound **9j'** in the crystal structure of tubulin.

DMSO-d_6): δ (ppm) 15.78, 47.79, 129.14, 124.32, 126.78, 128.38, 129.47, 130.09, 130.35, 131.63, 131.95, 136.21, 142.68, 148.61, 150.25, 187.73; LC-MS (ESI): 380.4 $(M + H)^+$.

4.2.8. (E)-3-(1-benzyl-2-(methylthio)-1H-imidazol-4-yl)-1-(4-phenoxyphenyl) prop-2-en-1-one (9e)

Yield: 44%; mp = 144–146 °C; ^{1}HNMR(300 MHz-DMSO-d_6): δ (ppm) 2.52 (s, 3H, SCH_3), 5.39 (s, 2H, CH_2), 7.05–7.08 (m, 2H, ArH), 7.08–7.11 (m, 2H, ArH), 7.11–7.15 (m, 2H, ArH), 7.23–7.31(m, 2H, ArH), 7.35–7.40(m, 2H, ArH), 7.44–7.51(m, 2H ArH), 7.51–7.56 (d, 1H, CH = CH, J = 15.3 Hz), 7.63–7.68 d, 1H, CH = CH, J = 15.3 Hz); ^{13}CNMR(75 MHz-DMSO-d_6): δ (ppm) 15.05, 47.38, 117.74, 118.83, 120.39, 125.19, 126.63, 128.16, 129.38, 130.79, 131.25, 131.58, 132.91, 133.98, 136.81, 148.34, 155.53, 161.55, 187.24; LC-MS (ESI): 427.3 $(M + Na)^+$.

4.2.9. (E)-3-(1-benzyl-2-(ethylthio)-1H-imidazol-4-yl)-1-(4-phenoxyphenyl) prop-2-en-1-one (9e')

Yield: 41%; mp = 127–129 °C; ^{1}HNMR (300 MHz-DMSO-d_6): δ (ppm)1.27–1.31 (t, 3H, CH_3, J = 7.2 Hz), 3.13–3.20 (q, 2H, SCH_2, J = 7.2 Hz), 5.42 (s, 2H, CH_2), 7.05–7.09 (m, 3H, ArH), 7.13–7.15 (m, 2H, ArH), 7.23–7.31 (m, 2H, ArH), 7.35–7.40 (m, 2H, ArH), 7.45–7.55 (m, 2H, ArH), 7.63–7.68 (d, 1H, CH = CH, J = 15.3 Hz), 8.03–8.05 (m, 3H, ArH); ^{13}CNMR(75 MHz-DMSO-d_6): δ (ppm), 15.52, 27.64, 47.40, 117.74, 119.00, 120.40, 125.20, 126.55, 128.13, 129.37, 129.41, 130.80, 131.26, 132.89, 134.07, 136.94, 147.14, 155.52, 161.56, 187.27; LC-MS (ESI):441.6 $(M + 1)^+$, 463.3 $(M + Na)^+$.

4.2.10. (E)-3-(1-benzyl-2-(methylthio)-1H-imidazol-4-yl)-1-(p-tolyl)prop-2-en-1-one (9f)

Yield: 79%; mp = 118–120 °C; ^{1}HNMR(300 MHz-DMSO-d_6): δ (ppm) 2.39(s, 3H, Toluene) 2.76 (s, 3H, SCH_3), 5.51 (s, 2H, CH_2), 7.14–7.17 (m, 2H, H_3 & H_5, p-tolyl), 7.30–7.43 (m, 5H,ArH), 7.50–7.55 (d, 1H, CH = CH, J = 15.3 Hz), 7.82–7.87 (d, 1H, CH = CH, J = 15.3 Hz), 7.93–7.96 (d, 2H, p-tolyl, H_2&H_6, J = 15.6 Hz), 8.40 (s, 1H, imidazole); ^{13}CNMR (75 MHz-DMSO-d_6): δ (ppm) 16.12, 21.67, 48.12, 126.79, 126.87, 127.13, 128.06, 128.55, 128.60, 129.52, 130.88, 131.88, 132.38, 135.63, 136.58, 147.42; LC-MS (ESI): 349.4 $(M + H)^+$.

4.2.11. (E)-3-(1-benzyl-2-(methylthio)-1H-imidazol-4-yl)-1-(naphthalen-2-yl)prop-2-en-1-one (9g)

Yield: 54%; mp = 189–191 °C; ^{1}HNMR(300 MHz-DMSO-d_6): δ (ppm) 2.51 (s, 3H, SCH_3), 5.56 (s, 2H, CH_2), 7.17–7.20 (m, 2H, ArH), 7.31–7.45 (m, 3H, ArH), 7.59–7.64 (d, 1H, CH = CH, J = 15.6 Hz), 7.66–7.73 (m, 2H, ArH), 8.01–8.14 (m, 5H, ArH) 8.79 (s, 1H, imidazole); ^{13}CNMR(75 MHz-DMSO-d_6): δ (ppm) 16.21, 48.19, 122.381, 124.41, 126.83, 127.54, 128.23, 128.50, 129.01, 129.29, 129.52, 130.03, 130.81, 132.00, 132.69, 135.01, 135.56, 135.83, 147.74, 188.42; LC-MS (ESI): 385.5 $(M + H)^+$.

4.2.12. (E)-3-(1-benzyl-2-(ethylthio)-1H-imidazol-4-yl)-1-(naphthalen-2-yl)prop-2-en-1-one (9g')

Yield: 57%; mp = 103–105 °C; ^{1}HNMR (300 MHz-DMSO-d_6): δ (ppm)1.28–1.32 (t, 3H, CH_3, J = 7.2 Hz), 3.14–3.22 (s, 2H, SCH_2, J = 7.2 Hz), 5.45 (s, 2H, CH_2), 7.10–7.12(m, 2H, ArH), 7.28–7.33(d, 1H, CH = CH, J = 15.6 Hz), (7.37–7.42 (m, 2H, ArH), 7.60–7.70 (m, 3H, ArH), 7.82–7.87 (, 1H, CH = CH, J = 15.6 Hz) , 7.99–8.03 (m, 2H, ArH), 8.099–8.12 (m, 2H, ArH); ^{13}CNMR(75 MHz-DMSO-d_6): δ (ppm), 15.57, 27.64, 47.46, 119.115, 124.50, 126.56, 127.42, 128.17, 128.88, 129.05, 129.40, 129.65, 129.97, 130.32, 131.53, 132.72, 134.36, 135.43, 136.94, 147.38, 188.65; LC-MS (ESI): 399.4 $(M + H)^+$.

4.2.13. (E)-1-([1,1′-biphenyl]-4-yl)-3-(1-benzyl-2-(ethylthio)-1H-imidazol-4-yl)prop-2-en-1-one (9h')

Yield: 51%; mp = 198–200 °C; ^{1}HNMR (300 MHz-DMSO-d_6): δ (ppm)1.26–1.31 (t, 3H, CH_3, J = 7.2 Hz), 3.24–3.31 (q, 2H, SCH_2, J = 7.2 Hz), 5.54 (s, 2H, CH_2), 7.32–7.51 (m, 6H, ArH), 7.52–7.60 (d, 1H, CH = CH, J = 15.6 Hz), 7.732–7.88 (m, 3H, ArH), 7.88–7.93 (d, 1H, CH = CH, J = 15.6 Hz), 8.12–8.152 (d, 2H, J = 8.7 Hz), 8.262–8.42 (s, 1H, imidazole); ^{13}CNMR(75 MHz-DMSO-d_6): δ (ppm), 15.43, 28.47, 48.07, 126.72, 127.33, 127.45, 127.512, 128.42, 128.49, 129.37, 129.47, 129.572, 129.619, 131.944, 135.944, 135.54, 138.311, 145.103, 188.09; LC-MS (ESI): 425.3 $(M + H)^+$.

4.2.14. (E)-3-(1-benzyl-2-(methylthio)-1H-imidazol-4-yl)-1-(4-methoxyphenyl) prop-2-en-1-one (9i)

Yield: 71%; mp = 152–154 °C; ^{1}H NMR(300 MHz-DMSO-d_6): δ (ppm) 2.67 (s, 3H, CH_3), 3.86 (s, 3H, OCH_3), 5.27 (s, 2H, CH_2), 6.90–6.93 (d, 2H, ArH, J = 8.7 Hz), 7.11–7.13 (d, 2H, ArH, J = 6.9 Hz), 7.26–7.38 (m, 4H, ArH), 7.56–7.62 (d, 1H, HC = CH, J = 15.3 Hz), 7.70 (s, 1H, imidazole), 7.85–7.88 (d, 2H, ArH, J = 8.7 Hz); ^{13}C NMR (75 MHz, $CDCl_3$): δ (ppm) 15.56, 47.89, 55.48, 113.79, 118.93, 126.37, 128.08, 128.54, 129.10, 130.59, 130.92, 131.39, 132.70, 135.46, 148.65, 163.37, 187.60; LC-MS(ESI): 365.4 $(M + H)^+$, 387.4 $(M + Na)^+$.

4.2.15. (E)-3-(1-benzyl-2-(ethylthio)-1H-imidazol-4-yl)-1-(4-methoxyphenyl) prop-2-en-1-one (9i')

Yield: 78%; mp = 143–145 °C; ^{1}H NMR(300 MHz-DMSO-d_6): δ (ppm) 1.35–1.39 (t, 3H, CH_3, J = 7.3 Hz), 3.16–3.23 (q, 2H, CH_2, J = 7.3 Hz), 3.86 (s, 3H, OCH_3), 5.30 (s, 2H, CH_2), 6.90–6.93 (d, 2H, ArH, J = 8.7 Hz), 7.09–7.12 (d, 2H, ArH, J = 7.2 Hz), 7.26–7.38 (m, 4H, ArH), 7.56–7.61 (d, 1H, HC = CH, J = 15.3 Hz), 7.71 (s, 1H, imidazole), 7.85–7.88 (d, 2H, ArH, J = 9 Hz); ^{13}C NMR (75 MHz, $CDCl_3$): δ (ppm) 15.03, 27.99, 47.91, 55.48, 113.79, 118.94, 126.32, 128.02, 128.68, 129.07, 130.59, 130.93, 131.22, 132.91, 135.66, 147.62, 163.37, 187.66; LC-MS(ESI): 379.4 $(M + H)^+$.

4.2.16. (E)-3-(1-benzyl-2-(methylthio)-1H-imidazol-4-yl)-1-(3,4,5-trimethoxyphenyl)prop-2-en-1-one (9j)

Yield: 81%; mp = 171–173 °C; ^{1}H NMR(300 MHz-DMSO-d_6): δ (ppm) 2.67 (s, 3H, CH_3), 3.86 (s, 6H, OCH_3), 3.91 (s, 3H, OCH_3), 5.28 (s, 2H, CH_2), 7.11–7.13 (t, 3H, ArH, J = 6.6 Hz), 7.18–7.23 (d, 1H, HC = CH, J = 15.6 Hz), 7.28–7.38 (m, 3H, ArH), 7.60–7.66 (d, 1H, HC = CH, J = 15.6 Hz), 7.71 (s, 1H, imidazole); ^{13}C NMR (75 MHz, $CDCl_3$): δ (ppm) 15.45, 47.94, 56.35, 60.96, 105.82, 118.21, 126.27, 128.10, 129.13, 129.43, 131.25, 133.36, 133.57, 135.39, 142.43, 149.21, 153.09, 188.05; LC-MS(ESI): 425.4 $(M + H)^+$, 447.4 $(M + Na)^+$.

4.2.17. (E)-3-(1-benzyl-2-(ethylthio)-1H-imidazol-4-yl)-1-(3,4,5-trimethoxyphenyl)prop-2-en-1-one (9j')

Yield: 61%; mp = 82–84 °C; ^{1}H NMR(300 MHz-DMSO-d_6): δ (ppm) 1.35–1.40 (t, 3H, CH_3, J = 7.3 Hz), 3.17–3.24 (q, 2H, CH_2, J = 7.3 Hz), 3.87 (s, 6H, OCH_3), 3.92 (s, 3H, OCH_3), 5.32 (s, 2H, CH_2), 7.10–7.13 (d, 4H, ArH, J = 6.9 Hz), 7.18–7.24 (d, 1H, HC = CH, J = 15.3 Hz), 7.29–7.39 (m, 3H, ArH), 7.61–7.66 (d, 1H, HC = CH, J = 15.3 Hz), 7.73 (s, 1H, imidazole); ^{13}C NMR (75 MHz, CDCl3): δ (ppm) 15.00, 27.91, 47.98, 56.36, 60.97, 105.83, 118.31, 126.24, 128.05, 129.10, 129.52, 131.08, 133.36, 133.62, 135.55, 142.43, 148.19, 153.10, 188.10; LC-MS (ESI): 439.5 $(M + H)^+$.

4.3. Synthesis of (E)-methyl 1-benzyl-5-(3-oxo-3-(3,4,5-trimethoxyphenyl)prop-1-en-1-yl)-1H-imidazole-2-sulfinate (9k)

Compound **9j** (300 mg, 0.7 mmol) was dissolved in THF (6 ml) and 1.5 g oxone in THF/water was added. The mixture was stirred at room temperature for 3 h, after evaporation of THF, the residue was washed with water and recrystallized in ethanol.

Yield: 87%; mp = 170–172 °C; ^{1}H NMR(300 MHz-DMSO-d_6): δ (ppm) 3.87 (s, 3H, OCH_3), 3.88 (s, 6H, OCH_3), 5.86 (s, 2H, CH_2), 7.15–7.18 (d, 2H, ArH, J = 8.4 Hz), 7.29–7.32 (m, 1H, ArH), 7.33–7.36 (d, 2H, ArH, J = 6.9 Hz), 7.37–7.42 (m, 2H, ArH), 7.51–7.56 (d, 1H, HC = CH, J = 15.3 Hz), 7.92–7.97 (d, 1H, HC = CH, J = 15.3 Hz); ^{13}CNMR (75 MHz-DMSO-d_6): δ (ppm), 43.55, 48.35, 56.69, 60.68, 106.71, 124.38, 126.64, 128.16, 128.35, 129.38, 131.62, 132.83, 133.75, 136.62, 142.76, 145.75, 153.40; LC-MS (ESI): 457.5 $(M + H)^+$, 479.4 $(M + Na)^+$.

4.4. Biological evaluation

4.4.1. Antiproliferative activity assay

To evaluate the antiproliferative activity, several human cancer cell lines, including A549 (adenocarcinoma human alveolar basal epithelial cells), MCF-7 (human breast cancer cells), MCF-7/MX (mitoxantrone resistant human breast cancer cells), and HEPG2 (human hepatocellular carcinoma cells) were grown in RPMI complete culture medium and then with a density of 5 × 10^3 cells/mL of the culture medium were seeded into 96-well plates and incubated at 37 °C in a 5% CO_2 incubator. After 24 h, the culture medium was substituted with a medium having positive control CA-4 as well as diverse concentrations of new synthesized compounds and RPMI as the negative control. After incubation at 37 °C for 48 h, the cell viability was determined using the MTT assay. The IC_{50} was defined as the compound concentration required to inhibit cell proliferation by 50%. The data were analyzed with GraphPad Prism [47].

4.4.2. Tubulin polymerization assay

Tubulin polymerization assay was done by using a commercial kit (cytoskeleton, cat. #BK011P). In brief, tubulin was suspended in ice-cold G-PEM buffer (80 mM PIPES, 2 mM $MgCl_2$, 0.5 mM EGTA, 1 mM GTP, 20% (v/v) glycerol) and added to wells on a 96-well plate containing **9g**, **9j** and **9j'** (at 50 and 100 μM concentration), Paclitaxel at 3 μM concentration, CA4 at 5 μM concentration and control (no drug), then Samples were mixed well, and tubulin polymerization was monitored by excitation at 360 nm and emission at 420 nm for 60 min at 1 min intervals [7].

4.4.3. Cell cycle analysis using flow cytometry

A549 cells were seeded into 6-well plates (2.5 × 10^5 cells/well) for 24 h, then treated with different concentrations of compounds 9j' and 9g and vehicle alone (0.05% DMSO) and were incubated for 48 h. After the cells were washed with PBS and fixed with 70% ethanol, then washed

twice with PBS, and then incubated for 0.5 h at 37C in a PBS solution containing RNase A (0.1 mg/mL) and propidium iodide (PI). The results were acquired and analyzed using Flowjo software [53].

4.4.4. Apoptosis analysis

The A549 cells in 6-well plates (2.5×10^5 cells/well) were seeded for 24 h. Then the medium was replaced with a complete medium containing different concentrations of compound **9j'**. After incubation for 24 h at 37 °C, the treated and untreated cells were harvested and washed with cold PBS. These cells were incubated with annexin V-FITC and PI (20 min) at room temperature. The samples were detected by a flow cytometer (Beckman Coulter), and the results were analyzed by Flowjo analysis software [53].

4.4.5. Molecular modeling

The mode of interaction between synthesized ligands and tubulin was examined by docking using MOE software. The x-ray crystal structure of tubulin (PDB ID:4O2B) was downloaded from the Protein Data Bank (PDB). 2D structure of the compounds was prepared in Chem Draw Ultra 8.0 software and 3D structure was achieved using Hyperchem 7 software through molecular mechanic force filed pre-optimization and then by AM1 semiempirical calculation. Compounds were docked into the binding site of tubulin by MOE software. The docking simulations were performed using triangle matcher placement algorithm and London dG scoring function and force field as the refinement process. The top-score docking poses were selected for the last ligand-target interaction analysis by the LigX module (in MOE Software). Validation of the docking manner was first evaluated by docking the co-crystalized ligand into the tubulin binding site [32].

Authors contributions

Sara Rahimzadeh Oskuei: Synthesis and doing MTT test. Salimeh Mirzaei: Synthesis and doing MTT test. Mohammad Reza Jafari-Nik: Synthesis. Farzin Hadizadeh: Docking studies. Farhad Eisvand: doing MTT test. Fatemeh Mosaffa: Supervision the biological tests. Razieh Ghodsi: Design and supervision the synthesis and biological tests.

Declaration of Competing Interest

The authors declare that they have no known competing financial interests or personal relationships that could have appeared to influence the work reported in this paper.

Acknowledgment

We thank the research deputy of Mashhad university of medical sciences for the financial support of this study (as part of the thesis of Sara Rahimzadeh Oskuee).

Appendix A. Supplementary data

Supplementary data to this article can be found online at https://doi.org/10.1016/j.bioorg.2021.104904.

References

[1] S. Giordano, A. Petrelli, From single-to multi-target drugs in cancer therapy: when aspecificity becomes an advantage, Curr. Med. Chem. 15 (5) (2008) 422–432.
[2] K. Nepali, S. Sharma, M. Sharma, P. Bedi, K. Dhar, Rational approaches, design strategies, structure activity relationship and mechanistic insights for anticancer hybrids, Eur. J. Med. Chem. 77 (2014) 422–487.
[3] M. Yousefian, R. Ghodsi, Structure–activity relationship studies of indolin-2-one derivatives as vascular endothelial growth factor receptor inhibitors and anticancer agents, Arch. Pharm. 353 (12) (2020) 2000022.
[4] M.A. Jordan, L. Wilson, Microtubules as a target for anticancer drugs, Nat. Rev. Cancer 4 (4) (2004) 253–265.
[5] H.Y. Kueh, T.J. Mitchison, Structural plasticity in actin and tubulin polymer dynamics, Science 325 (5943) (2009) 960–963.
[6] Y.V. Voitovich, E.S. Shegravina, N.S. Sitnikov, V.I. Faerman, V.V. Fokin, H.-G. Schmalz, et al., Synthesis and biological evaluation of furanoallocolchicinoids, J. Med. Chem. 58 (2) (2015) 692–704.
[7] F.S. Behbahani, J. Tabeshpour, S. Mirzaei, S. Golmakaniyoon, Z. Tayarani-Najaran, A. Ghasemi, et al., Synthesis and biological evaluation of novel benzo [c] acridine-diones as potential anticancer agents and tubulin polymerization inhibitors, Arch. Pharm. 352 (6) (2019) 1800307.
[8] V. Bobba, V. Nanavaty, N.D. Idippily, A. Zhao, B. Li, B. Su, Synthesis and biological evaluation of selective tubulin inhibitors as anti-trypanosomal agents, Bioorg. Med. Chem. 25 (12) (2017) 3215–3222.
[9] M. Driowya, J. Leclercq, V. Verones, A. Barczyk, M. Lecoeur, N. Renault, et al., Synthesis of triazoloquinazolinone based compounds as tubulin polymerization inhibitors and vascular disrupting agents, Eur. J. Med. Chem. 115 (2016) 393–405.
[10] S.D. Guggilapu, G. Lalita, T.S. Reddy, S.K. Prajapti, A. Nagarsenkar, S. Ramu, et al., Synthesis of C5-tethered indolyl-3-glyoxylamide derivatives as tubulin polymerization inhibitors, Eur. J. Med. Chem. 128 (2017) 1–12.
[11] L. Huang, M. Liu, S. Man, D. Ma, D. Feng, Z. Sun, et al., Design, synthesis and bio-evaluation of novel 2-aryl-4-(3, 4, 5-trimethoxy-benzoyl)-5-substituted-1, 2, 3-triazoles as the tubulin polymerization inhibitors, Eur. J. Med. Chem. 186 (2020), 111846.
[12] Y. Pang, J. Yan, B. An, L. Huang, X. Li, The synthesis and evaluation of new butadiene derivatives as tubulin polymerization inhibitors, Bioorg. Med. Chem. 25 (12) (2017) 3059–3067.
[13] R. Romagnoli, P.G. Baraldi, M.K. Salvador, D. Preti, M. Aghazadeh Tabrizi, A. Brancale, et al., Discovery and optimization of a series of 2-aryl-4-amino-5-(3′, 4′, 5′-trimethoxybenzoyl) thiazoles as novel anticancer agents, J. Med. Chem. 55 (11) (2012) 5433–5445.
[14] S. Sana, R. Tokala, D.M. Bajaj, N. Nagesh, K.K. Bokara, G. Kiranmai, et al., Design and synthesis of substituted dihydropyrimidinone derivatives as cytotoxic and tubulin polymerization inhibitors, Bioorg. Chem. 93 (2019), 103317.
[15] N. Shankaraiah, S. Nekkanti, U.R. Brahma, N.P. Kumar, N. Deshpande, D. Prasanna, et al., Synthesis of different heterocycles-linked chalcone conjugates as cytotoxic agents and tubulin polymerization inhibitors, Bioorg. Med. Chem. 25 (17) (2017) 4805–4816.
[16] E. Karimikia, J. Behravan, A. Zarghi, M. Ghandadi, S.O. Malayeri, R. Ghodsi, Colchicine-like β-acetamidoketones as inhibitors of microtubule polymerization: Design, synthesis and biological evaluation of in vitro anticancer activity, Iran. J. Basic Med. Sci. 22 (10) (2019) 1138.
[17] Y. Yin, B.-P. Lian, Y.-Z. Xia, Y.-Y. Shao, L.-Y. Kong, Design, synthesis and biological evaluation of resveratrol-cinnamoyl derivates as tubulin polymerization inhibitors targeting the colchicine binding site, Bioorg. Chem. 93 (2019), 103319.
[18] G. De Martino, M.C. Edler, G. La Regina, A. Coluccia, M.C. Barbera, D. Barrow, et al., New arylthioindoles: Potent Inhibitors of tubulin polymerization. 2. Structure–activity relationships and molecular modeling studies, J. Med. Chem. 49 (3) (2006) 947–954.
[19] G. Wang, C. Li, L. He, K. Lei, F. Wang, Y. Pu, et al., Design, synthesis and biological evaluation of a series of pyrano chalcone derivatives containing indole moiety as novel anti-tubulin agents, Bioorg. Med. Chem. 22 (7) (2014) 2060–2079.
[20] S. Messaoudi, B. Tréguier, A. Hamze, O. Provot, J.-F. Peyrat, J.R. De Losada, et al., Iso combretastatins A versus combretastatins A: The forgotten iso CA-4 isomer as a highly promising cytotoxic and antitubulin agent, J. Med. Chem. 52 (14) (2009) 4538–4542.
[21] B. Zhang, D. Duan, C. Ge, J. Yao, Y. Liu, X. Li, et al., Synthesis of xanthohumol analogues and discovery of potent thioredoxin reductase inhibitor as potential anticancer agent, J. Med. Chem. 58 (4) (2015) 1795–1805.
[22] J. Chen, C.-M. Li, J. Wang, S. Ahn, Z. Wang, Y. Lu, et al., Synthesis and antiproliferative activity of novel 2-aryl-4-benzoyl-imidazole derivatives targeting tubulin polymerization, Bioorg. Med. Chem. 19 (16) (2011) 4782–4795.
[23] S. Ducki, D. Rennison, M. Woo, A. Kendall, J.F.D. Chabert, A.T. McGown, et al., Combretastatin-like chalcones as inhibitors of microtubule polymerization. Part 1: Synthesis and biological evaluation of antivascular activity, Bioorg. Med. Chem. 17 (22) (2009) 7698–7710.
[24] M.L. Edwards, D.M. Stemerick, P.S. Sunkara, Chalcones: a new class of antimitotic agents, J. Med. Chem. 33 (7) (1990) 1948–1954.
[25] D. Kumar, N.M. Kumar, K. Akamatsu, E. Kusaka, H. Harada, T. Ito, Synthesis and biological evaluation of indolyl chalcones as antitumor agents, Bioorg. Med. Chem. Lett. 20 (13) (2010) 3916–3919.
[26] W.D. Seo, J.H. Kim, J.E. Kang, H.W. Ryu, M.J. Curtis-Long, H.S. Lee, et al., Sulfonamide chalcone as a new class of α-glucosidase inhibitors, Bioorg. Med. Chem. Lett. 15 (24) (2005) 5514–5516.
[27] G. Wang, Z. Peng, J. Zhang, J. Qiu, Z. Xie, Z. Gong, Synthesis, biological evaluation and molecular docking studies of aminochalcone derivatives as potential anticancer agents by targeting tubulin colchicine binding site, Bioorg. Chem. 78 (2018) 332–340.
[28] J. Kode, J. Kovvuri, B. Nagaraju, S. Jadhav, M. Barkume, S. Sen, et al., Synthesis, biological evaluation, and molecular docking analysis of phenstatin based indole linked chalcones as anticancer agents and tubulin polymerization inhibitors, Bioorg. Chem. 105 (2020), 104447.
[29] M.T. Konieczny, A. Bułakowska, D. Pirska, W. Konieczny, A. Skladanowski, M. Sabisz, et al., Structural factors affecting affinity of cytotoxic oxathiole-fused chalcones toward tubulin, Eur. J. Med. Chem. 89 (2015) 733–742.
[30] L. Li, S. Jiang, X. Li, Y. Liu, J. Su, J. Chen, Recent advances in trimethoxyphenyl (TMP) based tubulin inhibitors targeting the colchicine binding site, Eur. J. Med. Chem. 151 (2018) 482–494.

[31] H. Mirzaei, S. Emami, Recent advances of cytotoxic chalconoids targeting tubulin polymerization: Synthesis and biological activity, Eur. J. Med. Chem. 121 (2016) 610–639.
[32] S. Mirzaei, F. Hadizadeh, F. Eisvand, F. Mosaffa, R. Ghodsi, Synthesis, structure-activity relationship and molecular docking studies of novel quinoline-chalcone hybrids as potential anticancer agents and tubulin inhibitors, J. Mol. Struct. 1202 (2020), 127310.
[33] F. Sultana, S.R. Bonam, V.G. Reddy, V.L. Nayak, R. Akunuri, S.R. Routhu, et al., Synthesis of benzo [d] imidazo [2, 1-b] thiazole-chalcone conjugates as microtubule targeting and apoptosis inducing agents, Bioorg. Chem. 76 (2018) 1–12.
[34] B. Wang, L.-R. Wang, L.-L. Liu, W. Wang, R.-J. Man, D.-J. Zheng, et al., A novel series of benzothiazepine derivatives as tubulin polymerization inhibitors with anti-tumor potency, Bioorg. Chem. 108 (2021), 104585.
[35] G. Wang, W. Liu, Z. Gong, Y. Huang, Y. Li, Z. Peng, Design, synthesis, biological evaluation and molecular docking studies of new chalcone derivatives containing diaryl ether moiety as potential anticancer agents and tubulin polymerization inhibitors, Bioorg. Chem. 95 (2020), 103565.
[36] F. Xu, W. Li, W. Shuai, L. Yang, Y. Bi, C. Ma, et al., Design, synthesis and biological evaluation of pyridine-chalcone derivatives as novel microtubule-destabilizing agents, Eur. J. Med. Chem. 173 (2019) 1–14.
[37] C. Zhu, Y. Zuo, R. Wang, B. Liang, X. Yue, G. Wen, et al., Discovery of potent cytotoxic ortho-aryl chalcones as new scaffold targeting tubulin and mitosis with affinity-based fluorescence, J. Med. Chem. 57 (15) (2014) 6364–6382.
[38] A. Assadieskandar, M. Amini, S.N. Ostad, G.H. Riazi, T. Cheraghi-Shavi, B. Shafiei, et al., Design, synthesis, cytotoxic evaluation and tubulin inhibitory activity of 4-aryl-5-(3, 4, 5-trimethoxyphenyl)-2-alkylthio-1H-imidazole derivatives, Bioorg. Med. Chem. 21 (10) (2013) 2703–2709.
[39] C. Lamberth, R. Dumeunier, S. Trah, S. Wendeborn, J. Godwin, P. Schneiter, et al., Synthesis and fungicidal activity of tubulin polymerisation promoters. Part 3: imidazoles, Bioorg. Med. Chem. 21 (1) (2013) 127–134.
[40] S.P. Shaik, M. Vishnuvardhan, F. Sultana, A.S. Rao, C. Bagul, D. Bhattacharjee, et al., Design and synthesis of 1, 2, 3-triazolo linked benzo [d] imidazo [2, 1-b] thiazole conjugates as tubulin polymerization inhibitors, Bioorg. Med. Chem. 25 (13) (2017) 3285–3297.
[41] Q. Wang, K.E. Arnst, Y. Wang, G. Kumar, D. Ma, H. Chen, et al., Structural modification of the 3, 4, 5-trimethoxyphenyl moiety in the tubulin inhibitor VERU-111 leads to improved antiproliferative activities, J. Med. Chem. 61 (17) (2018) 7877–7891.
[42] R. Singh, M. Sharma, P. Joshi, D.S. Rawat, Clinical status of anti-cancer agents derived from marine sources, Anti-Cancer Agents Med. Chem. (Formerly Current Medicinal Chemistry-Anti-Cancer Agents) 8 (6) (2008) 603–617.
[43] K. Nicolaou, J. Pfefferkorn, J. Xu, N. Winssinger, T. Ohshima, S. Kim, et al., Total synthesis and chemical biology of the sarcodictyins, Chem. Pharm. Bull. 47 (9) (1999) 1199–1213.
[44] F. Hadizadeh, R. Ghodsi, Synthesis of novel N-substituted imidazolecarboxylic acid hydrazides as monoamine oxidase inhibitors, Farmaco (Societa chimica italiana: 1989) 60 (3) (2005) 237–240.
[45] T. Abdizadeh, M.R. Kalani, K. Abnous, Z. Tayarani-Najaran, B.Z. Khashyarmanesh, R. Abdizadeh, et al., Design, synthesis and biological evaluation of novel coumarin-based benzamides as potent histone deacetylase inhibitors and anticancer agents, Eur. J. Med. Chem. 132 (2017) 42–62.
[46] R. Ghodsi, E. Azizi, A. Zarghi, Design, Synthesis and Biological Evaluation of4-(Imidazolylmethyl)-2-(4-methylsulfonyl phenyl)-Quinoline Derivatives as Selective COX-2 Inhibitors and In-vitro Anti-breast Cancer Agents, Iran. J. Pharm. Res.: IJPR 15 (1) (2016) 169–177.
[47] S. Golmakaniyoon, V.R. Askari, K. Abnous, A. Zarghi, R. Ghodsi, Synthesis, Characterization and In-vitro Evaluation of Novel Naphthoquinone Derivatives and Related Imines: Identification of New Anticancer Leads, Iran. J. Pharm. Res.: IJPR 18 (1) (2019) 16–29.
[48] F. Jafari, H. Baghayi, P. Lavaee, F. Hadizadeh, F. Soltani, H. Moallemzadeh, et al., Design, synthesis and biological evaluation of novel benzo- and tetrahydrobenzo-[h]quinoline derivatives as potential DNA-intercalating antitumor agents, Eur. J. Med. Chem. 164 (2019) 292–303.
[49] S.O. Malayeri, K. Abnous, A. Arab, M. Akaberi, S. Mehri, A. Zarghi, et al., Design, synthesis and biological evaluation of 7-(aryl)-2,3-dihydro-[1,4]dioxino[2,3-g] quinoline derivatives as potential Hsp90 inhibitors and anticancer agents, Bioorg. Med. Chem. 25 (3) (2017) 1294–1302.
[50] S.O. Malayeri, Z. Tayarani-Najaran, F.S. Behbahani, R. Rashidi, S. Delpazir, R. Ghodsi, Synthesis and biological evaluation of benzo[b]furo[3,4-e][1,4] diazepin-1-one derivatives as anti-cancer agents, Bioorg. Chem. 80 (2018) 631–638.
[51] Z. Rozmer, T. Berki, G. Maasz, P. Perjesi, Different effects of two cyclic chalcone analogues on redox status of Jurkat T cells, Toxicol. In Vitro: An International Journal Published in Association with BIBRA. 28 (8) (2014) 1359–1365.
[52] S. Mirzaei, M. Qayumov, F. Gangi, J. Behravan, R. Ghodsi, Synthesis and biological evaluation of oxazinonaphthalene-3-one derivatives as potential anticancer agents and tubulin inhibitors, Iran. J. Basic Med. Sci. 23 (11) (2020) 1388–1395.
[53] N. Shobeiri, M. Rashedi, F. Mosaffa, A. Zarghi, M. Ghandadi, A. Ghasemi, et al., Synthesis and biological evaluation of quinoline analogues of flavones as potential anticancer agents and tubulin polymerization inhibitors, Eur. J. Med. Chem. 114 (2016) 14–23.